ACS OMEGA

http://pubs.acs.org/journal/acsodf

Article

Structural Elucidation of Relevant Gibberellic Acid Impurities and *In Silico* Investigation of Their Interaction with Soluble Gibberellin Receptor GID1

Pierluigi Caboni,* Antonio Laus, Kodjo Eloh, Nikoletta G. Ntalli, Mattia Casula, Sabrina Di Giorgi, and Graziella Tocco*

Cite This: *ACS Omega* 2023, 8, 1957−1966

Read Online

ACCESS | Metrics & More | Article Recommendations | Supporting Information

ABSTRACT: Gibberellin derivatives are a family of tetracyclic diterpenoid plant hormones used in agriculture as plant growth regulators included in the European Directive 91/414. In the pesticide peer review process and to assess their toxicological relevance and product chemical equivalence, the European Food Safety Authority (EFSA) highlighted data gaps such as the identification of hydrolysis products and unknown impurities. The aspect of impurity characterization and quantitation is challenging and requires the use of hyphenated analytical techniques. In this regard, we used an LC-QTOF/MS and NMR analysis for the characterization of gibberellic acid impurities found in technical products. Gibberellic acid impurities such as gibberellin A1 (**GA_1**), 3-isolactone gibberellic acid (**iso-GA_3**), gibberellenic acid, 1α,2α-epoxygibberellin A3 (**2-epoxy- GA_3**), and (1α,2β,3α,4bβ,10β)-2,3,7-trihydroxy-1-methyl-8-methylenegibb-4-ene-1,10-dicarboxylic acid were identified and successfully characterized. Moreover, an *in silico* investigation on selected gibberellic acid impurities and derivatives and their interactions with a gibberellin insensitive dwarf1 (GID1) receptor has been carried out by means of induced fit docking (IFD), generalized-Born surface area (MM-GBSA), and metadynamics (MTD) experiments. A direct HPLC method with DAD and MS for the detection of gibberellic acid and its impurities in a technical sample has been developed. Moreover, by means of the *in silico* characterization of the GID1 receptor-binding pocket, we investigated the receptor affinity of the selected gibberellins, identifying compounds (**2**) and (**4**) as the most promising hit to lead compounds.

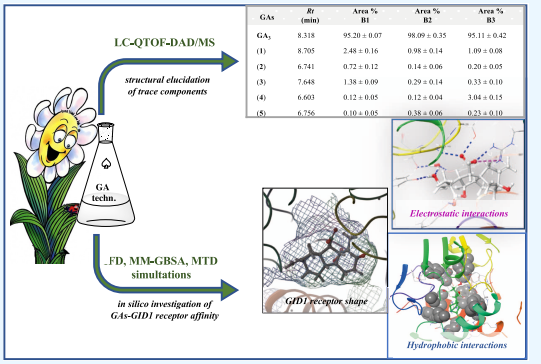

INTRODUCTION

Gibberellins (GAs) are phytohormones used as growth and development regulators agents. GAs are commercially produced by the fungi *Gibberella fujikuroi*.[1] Production of GAs is done by submerged fermentation in big tanks, yielding the broth that is then processed by organic solvent extraction in acidified pH and finally concentrated.[2] For the European Chemical Agency, gibberellic acid (**GA_3**), **GA_4**, **GA_7**, **GA_4**, and **GA_7** mixtures and potassium gibberellate are some of the compounds belonging to the gibberellin group.[3] In crop plants, GAs regulate shoot elongation and flowering in biennial photoperiodic plants.[4] In agriculture, GAs are used as plant regulators to stimulate cell division and elongation that affect leaves as well as stems, eventually involving fruit development and set as well as plant maturation and seed germination. Practically, GAs are applied to field crops, small fruits, vines, tree fruits, ornamental and shade trees, ornamental plants, shrubs, and vines. Nowadays, they are classified as biochemical pesticides as naturally occurring compounds with a nontoxic mode of action in target plants.[5] Gibberellic acid was included in Annex I to Directive 91/414/EEC on 1 September 2009, by the Commission Directive 2008/127/EC, pursuant to Article 24b of the Regulation (EC) No 2229/2004, and has subsequently been deemed to be approved under Regulation (EC) No 1107/2009, in accordance with Commission Implementing Regulation (EU) No 540/2011, as amended by Commission Implementing Regulation (EU) No 541/2011. In accordance with Article 25 (1) of Regulation (EC) No 2229/2004, the European Food Safety Authority (EFSA) has presented its conclusions on the peer review of the pesticide risk assessment of the active substance gibberellic acid (GA3).[5] Nowadays, the extension of its authorization for minor uses allows gibberellic acid to be employed in practical use.[6] Nonetheless, some data gaps within the field of identity, physicochemical properties, and methods of analysis were evidenced, with particular regard to the storage stability, the

Received: July 29, 2022
Accepted: November 14, 2022
Published: January 4, 2023

analytical method for relevant impurities analysis, and their mammalian toxicology.[7] Specifically, compared to the active ingredient, relevant impurities at a concentration greater than 0.1% are considered those compounds that may have pronounced toxic and phytotoxic characteristics or can be found as residues in food or the environment.[8]

To present and the best of our knowledge, there are few published studies on the determination of GA_3 and respective impurities in technical products.[9] Only Castillo and Martinez described a reversed-phase C_{18} HPLC procedure applied for the separation of GA_3 and GA_1 in the fermentation broth, while no impurities were identified.[4] Moreover, the current bibliography is focused on the analytical methods of identification of GAs as free substances rather than broth or plant extract components. In this regard, Lin and Stafford developed a method to separate 23 free GAs and their methyl esters by various chromatographic systems,[10] while Han et al. determined GA_3 in grapes by the high-performance liquid chromatography-tandem mass spectrometry (HPLC-MS) method.[11] Thus, the identification and quantitation of gibberellic acid impurities in technical pesticide batches represent an intense focus point for the pesticide manufacturing industry, particularly for the assessment of equivalence for applications for plant protection product authorization.

In the present paper, we addressed the problem of identification and characterization of active gibberellins and relative impurities of three commercially available batches (B1, B2, and B3) of technical gibberellic acid using high-performance liquid chromatography with diode array detection (HPLC−DAD) to determine GA peaks with high specificity and sensitivity. Then, hyphenated liquid chromatography quadrupole time-of-flight mass spectrometry (LC-QTOF-MS) allowed us to clearly identify each component of the sample under investigation. In fact, the combination of HPLC and high-resolution mass spectrometry is the ideal solution for the detection and identification of unknown substances, especially for the management of pesticide formulations. In addition, nuclear magnetic resonance (NMR) analysis provided further structural information.

For better structural confirmation, the detected impurities have been also synthesized as analytical standards for quantitation purposes. The molecular similarity of the impurities evidenced in the GA_3 batches prompted us to better investigate the structural basis of the phytohormonal activity of gibberellins. Although different protein factors might be involved in the GAs signaling, the nuclear receptor gibberellin insensitive dwarf1 (GID1) plays a key role in regulating many plants developing events by destabilization of the plant growth repressors DELLA proteins.[12] Thus, based on the recently resolved crystal structure of GID1,[13,14] we performed an *in silico* investigation to provide an accurate description of the ligand structural features essential for a better adaptation to the receptor. First, validation of the receptor model and the ligand−receptor interactions was carried out. The model was then applied to the investigation of GA_3 impurities by means of IFD, MM-GBSA, and MTD simulations to highlight the energetically more favorable ligand−receptor complexes related to a better adaptation to the GID1.

MATERIALS AND METHODS

Chemicals and Technical Products. Methanol, formic acid, trifluoroacetic acid, sodium sulfate, ethyl acetate, hydrogen chloride, sodium hydroxide, and hexane were obtained from Merck (Milan, Italy), while water was distilled with a Milli-Q Advantage A10 Water Purification System. Compounds (**3**) and (**4**) were obtained, respectively, from Merck (Milan, Italy) and Toronto Research Chemicals Inc (Canada). Compound (**1**) and other gibberellin analytical standards were kindly donated by Prof. Lewis Norman Mander. According to the literature,[15] gibberellin derivatives (**2**), (**3**), (**5**), and (**6**) were prepared as follows. Three different batches of gibberellic acid (purity >95%) were obtained from a local commercial retailer.

Experimental Chemistry. ^{1}H and ^{13}C NMR spectra were recorded on a Varian Unity INOVA 500 MHz spectrometer. High-resolution mass spectra were recorded using an Agilent 6520 Accurate-Mass Q-TOF LC/MS system.

Synthesis of (1S,4R,5bR,8S,10aS,11S,11aS,13R)-8,13-Dihydroxy-1-methyl-9-methylene-2-oxo-1,2,5b,6,7,8,9,10,11,11a-decahydro-4H-1,4:8,10a-dimethanoazuleno [1,2-d]oxepine-11-carboxylic acid (2). A solution of gibberellic acid (GA_3) (1.44 mmol) and sodium hydroxide (11.91 mmol) in water (250 mL) was stirred at room temperature for 90 min. Then, the reaction mixture was acidified to pH 3.0, extracted with ethyl acetate (40 mL x 5), and the combined organic layers dried over sodium sulfate, filtered, and concentrated under a vacuum to give compound (**2**) as a white solid. Yield (%) = 72. ^{1}H NMR (d_6-acetone, 500 MHz): δ 5.81 (dd, J = 5.4, 2.6 Hz, 1H), 4.93 (bs, 2H), 4.70 (t, J = 5.3 Hz, 1H), 4.29 (d, J = 5.3 Hz, 1H), 3.34 (dd, J = 6.1, 2.8 Hz, 1H), 2.68 (dt, J = 16.4, 3.1 Hz, 1H), 2.60 (d, J = 7.7 Hz 1H), 2.45 (d, J = 6.1 Hz, 1H), 2.30 (d, J = 16.4 Hz, 1H), 2.00−1.90 (m, 3H), 1.79−1.62 (m, 3H), 1.53−1.48 (m, 3H), 1.40−1.32 (m, 2H), 1.21 (td, J = 7.2, 1.6 Hz, 1H) ppm. ^{13}C NMR (d_6-acetone, 126 MHz): δ 176.66(C11-COOH), 175.12 (C2), 154.78 (C9), 151.00 (C5a), 113.72 (C5), 105.38 (C=CH_2), 78.11 (C4), 74.94 (C8), 73.98 (C13), 49.08 (C1), 48.87 (C11), 48.74 (C5b), 48.21 (C11a), 45.81 (C12), 45.42 (C10a), 39.08 (C10), 37.66 (C7), 18.49 (C6), 16.50 (CH_3) ppm. HRMS: calcd for $C_{19}H_{22}O_6NH_4$ $[M + NH_4]^+$: 364.1760, observed 364.1761.

Synthesis of (1S,2S,7S,9aR,10S,10aS)-2,7-Dihydroxy-1-methyl-8-methylene-2,5,6,7,8,9,10,10a-octahydro-1H-7,9a-methanobenzo[a]azulene-1,10-dicarboxylic acid (3). Gibberellic acid (GA_3) (1.44 mmol) was suspended in hydrazine monohydrate (2.25 mL) in water (250 mL), and the mixture was stirred for 30 min at 110 °C. Then, the reaction was cooled for 5 min in an ice bath, diluted in ice water, and acidified to pH 3.0 with concentrated hydrochloric acid. The aqueous phase was extracted with ethyl acetate (40 mL × 5), and the combined organic layers were treated with brine, dried over sodium sulfate, and concentrated under a vacuum. Compound (**3**) was obtained as a white solid. Yield (%) = 49. ^{1}H NMR (d6-acetone, 500 MHz): 10.61 (bs, 1H), 6.33 (d, J = 9.7 Hz, 1H), 5.92 (dd, J = 9.7, 5.6 Hz, 1H), 5.15 (dd, J = 3.6, 1.9 Hz, 1H), 4.92 (s, 1H), 4.34 (d, J = 5.6 Hz, 1H), 3.73 (d, J = 8.5 Hz, 1H), 3.58 (dd, J = 8.6, 4.4 Hz, 1H), 2.63 (dd, J = 16.3, 6.5 Hz, 1H), 2.52 (d, J = 16.5 Hz, 1H), 2.24−2.14 (m, 3H), 1.97 (s, 1H), 1.79 − 1.60 (m, 3H), 1.29 (s, 3H), 1.21 (dd, J = 8.1, 6.2 Hz, 1H). ppm. ^{13}C NMR (d_6-acetone, 126 MHz): δ 175.36(C1-COOH), 174.91(C10-COOH), 155.41 (C8), 138.95 (C4a), 129.65 (C3), 127.37 (C4b), 123.22 (C4), 104.76 (C=CH_2), 78.23 (C7), 68.99 (C2), 55.52 (C1), 52.24 (C9a), 49.19 (C11), 48.91(C10a), 47.72 (C6), 39.84 (C9),

https://doi.org/10.1021/acsomega.2c04743
ACS Omega 2023, 8, 1957−1966

39.15 (C10), 20.32 (C5), 19.60 ($\underline{C}H_3$) ppm. HRMS: calcd for $C_{19}H_{22}O_6$ NH_4 $[M + NH_4]^+$: 364.1760, observed 364.1761.

*Synthesis of (1S,2R,3R,4bR,7S,9aS,10S,10aS)-2,3,7-Trihydroxy-1-methyl-8- methylene-2,3,4b,5,6,7,8,9,10,10a-decahydro-1H-7,9a-methanobenzo[a]azulene-1,10-dicarboxylic acid (**5**).* Gibberellic acid (0.5 g, 1.44 mmol) and sodium hydroxide (0.24 mg, 5.93 mmol) were dissolved in water (57 mL) and stirred at room temperature for 18 h. Then, the mixture was cooled in an ice bath and quenched with hydrogen chloride to pH 2.0. The reaction was extracted with ethyl acetate (40 mL × 5), dried over sodium sulfate, and concentrated. The residue was then triturated with hexanes to afford a known compound (**5**) as a white solid. Yield (%) = 63. ^{1}H NMR (d_6-DMSO, 500 MHz): δ 12.27 (s, 1H), 5.20 (q, J = 2.8 Hz, 1H), 5.05 (s, 1H), 4.99 (p, J = 1.6 Hz, 1H), 4.86 (d, J = 2.3 Hz, 1H), 4.73 (s, 1H), 3.91−3.82 (m, 1H), 3.69 (d, J = 3.0 Hz, 1H), 2.85 (d, J = 6.3 Hz, 1H), 2.74 (d, J = 6.0 Hz, 1H), 2.32 (d, J = 6.3 Hz, 1H), 2.12 (dd, J = 16.2, 2.6 Hz, 1H), 1.81 (d, J = 10.7 Hz, 1H), 1.62 (dd, J = 10.9, 2.7 Hz, 1H), 1.59−1.47 (m, 2H), 1.43 − 1.34 (m, 1H), 1.30 (dd, J = 10.9, 2.5 Hz, 1H), 1.14 (s, 3H) ppm. ^{13}C NMR (d_6-acetone, 126 MHz): δ 176.67 (C1-$\underline{C}$OOH),175.81(C10-$\underline{C}$OOH), 155.39 (C8), 142.89 (C4a), 115.30 (C4), 105.06 (C=$\underline{C}H_2$), 78.35 (C7), 74.84 (C2), 70.88 (C3), 49.68 (C10), 49.31 (C1), 48.53 (C4b), 46.99 (C10a), 46.41 (C11), 46.25 (C9a), 39.25 (C9), 27.84 (C9), 20.83(C5), 18.46 ($\underline{C}H_3$) ppm. HRMS(ESI): m/z calcd for $C_{19}H_{24}O_7Na$ $[M + Na]^+$: 387.1420, found, 387.1420.

*Synthesis of (7S,9aS,10R)-7-Hydroxy-1-methyl-8-methylene-4b,6,7,8,9,10-hexahydro-5H-7,9a-methanobenzo[a]-azulene-10-carboxylic acid (**6**).* Gibberellic acid (0.5 g, 1.44 mmol) was dissolved in hydrochloric acid (1.2 M, 7.1 mL) and heated for 3 h at 65 °C. Then, the reaction was cooled, and the solid precipitate was filtered and washed with water affording compound (**6**), as a white solid.^{1}H NMR (d_6-acetone, 500 MHz): δ 7.11 (t, J = 7.4 Hz, 1H), 6.99 (d, J = 7.6 Hz, 1H), 6.95 (d, J = 7.3 Hz, 1H), 5.01 (td, J = 2.7, 1.2 Hz, 1H), 4.77−4.67 (m, 1H), 3.98 (s, 1H), 2.88 (dd, J = 12.5, 5.1 Hz, 1H), 2.32−2.23 (m, 3H), 2.21 (s, 3H), 1.95 (td, J = 12.3, 5.1 Hz, 2H), 1.91−1.83 (m, 2H), 1.68 (ddd, J = 12.0, 4.9, 2.4 Hz, 1H), 1.55 (dd, J = 12.8, 5.2 Hz, 1H) ppm.^{13}C NMR (d_6-acetone, 500 MHz): δ 171.73 ($\underline{C}$OOH), 155.26 (C8), 144.87 (C4a), 138.93 (C10a), 134.97 (C1), 128.50 (C2), 127.05 (C3), 119.43 (C4), 102.16 (C=$\underline{C}H_2$), 79.74 (C7), 54.39 (C10), 52.97 (C4b), 51.94 (C11), 48.34 (C9), 39.89 (C6), 34.07 (C9a), 21.95 (C5), 19.09 ($\underline{C}H_3$) ppm. HRMS(ESI): m/z calcd for $C_{18}H_{20}O_3Na$ $[M + Na]^+$: 307.1310, found, 307.1309.

Apparatus and Chromatography. *HPLC−DAD Analysis.* GA_3 and related compounds were analyzed by reverse-phase LC on an Agilent 1260 series LC system fitted with a diode array detector. An Agilent Poroshell 120 EC-C18 4 μ 4.6 × 100 mm (Agilent, Santa Clara, CA) or a Kinetex 5 μ EVO C18 100A 150 × 2.1 mm column was used. The LC conditions were as follows: flow rate, 1.0 mL/min; solvent A, 0.1% aqueous formic acid containing ammonium formate 5 mM; solvent B, methanol; and the gradient was from 10 to 80% B over 15 min and kept in these conditions for 5 min. On the other hand, an isocratic method consisting of solvent A aqueous 0.1% TFA and methanol was used at a solvent ratio of 70:30 v/v for confirmation of peaks.

HPLC-QTOF/MS Analysis. Samples (8 μL) were then analyzed by ESI in positive and negative modes using an Agilent 6520 Time of Flight (TOF) MS. Mass spectral data were acquired in the range of 100−1500 m/z with an acquisition rate of 1.35 spectra/s, averaging 10,000 transients. The source parameters were adjusted as follows: drying gas temperature 250 °C, drying gas flow rate 5 L/min, nebulizer pressure 45 psi, and fragmentor voltage 150 V. The eluting compounds were analyzed and quantified using Agilent MassHunter Workstation software. Levels of GA3, (1), (2), and (3) in commercial technical samples were measured by HPLC−DAD and HPLC-QTOF/MS analysis and calculated based on linear calibration functions considering the dilution factors. The contents of GAs in the technical product were expressed as mass percentages.

Standard and Working Solutions. Six aliquots of 10 mg of the GA formulations B1, B2, and B3 of the test substances were transferred in 10 mL volumetric flasks and dissolved in methanol after ultrasonication in a water bath. The volume was then adjusted to 10 mL. *Standard Curves and Linearity*. Six stock solutions of GA_3, (**1**), (**2**), (**3**), (**4**), and (**5**) were prepared at 1000 mg/L using methanol as a solvent. Standard working solutions of GAs were prepared by diluting the standard solution with the mobile phase (water/methanol 9:1 v/v). Intermediary mixed standard solutions were prepared daily by diluting stock solutions with methanol. Levels of calibration for all impurities including a blank, were 1, 5, 10, 20, 50, and 100 mg/L, respectively. All standard solutions were stored in the dark at −20 °C until use. Calibration curves were created by plotting the concentration of each compound against the standard UV of the MS peak area. Simple linear regression analysis was performed to calculate the slope and intercept. The correlation coefficient (r) for each gibberellin was also determined. *Repeatability*. To evaluate precision, the repeatability of the HPLC−DAD used and the analytical method proposed was determined. Between-day repeatability was calculated by performing six injections of the same standard at 10, 50, 100, 500, and 1000 μg/L for six consecutive days.

Construction of the Simulated Systems. The crystal structures of the active gibberellin insensitive dwarf1 (GID1) bound to **GA3** agonist (PDB ID, 2ZSH) and **GA4** (PDB ID, 2ZSI) were obtained at 1.80 Å for both 2ZSH and 2ZSI from the RCSB database. The protein preparation wizard tool included in the Maestro molecular modeling suite was used to prepare and refine each structure at pH 7.0 ± 0.5, employing default parameters.[16−20] The compounds under study were prepared and docked in the previously cited GID1 receptors by means of the Schrödinger Release 2020-1 (Schrödinger Release 2020-1: Maestro, Schrödinger, LLC, New York, NY) with the OPLS3e force field. The gibberellins GA_1 (**1**), iso-GA3 (**2**), gibberellenic acid (**3**), 1,2-epoxy-GA_3 (**4**), (1α,2β,3α,4bβ,10β)-2,3,7-trihydroxy-1-methyl-8-methylene-gibb-4-ene-1,10-dicarboxylic acid (**5**), and 9-βH epiallogibberic acid (**6**) were, prior equilibration, cross-docked in the GID1 receptor-binding areas using the LigPrep module to construct the compounds at pH 7.0 ± 0.5. Each compound was assigned a net charge by the Epik module before the GID1 model was prepared by the induced fit docking (IFD) protocol of the Schrödinger suite. A grid box of docking, important for binding compounds of comparable size, was located no more than 5 Å from the crystal ligand. Dockings were then performed using a standard protocol whereby conformations of the ligand were screened for clashes with the protein and subsequently refined by allowing flexibility of the side chains in the binding in the presence of an implicit membrane and solvent.[19−24]

https://doi.org/10.1021/acsomega.2c04743
ACS Omega 2023, 8, 1957−1966

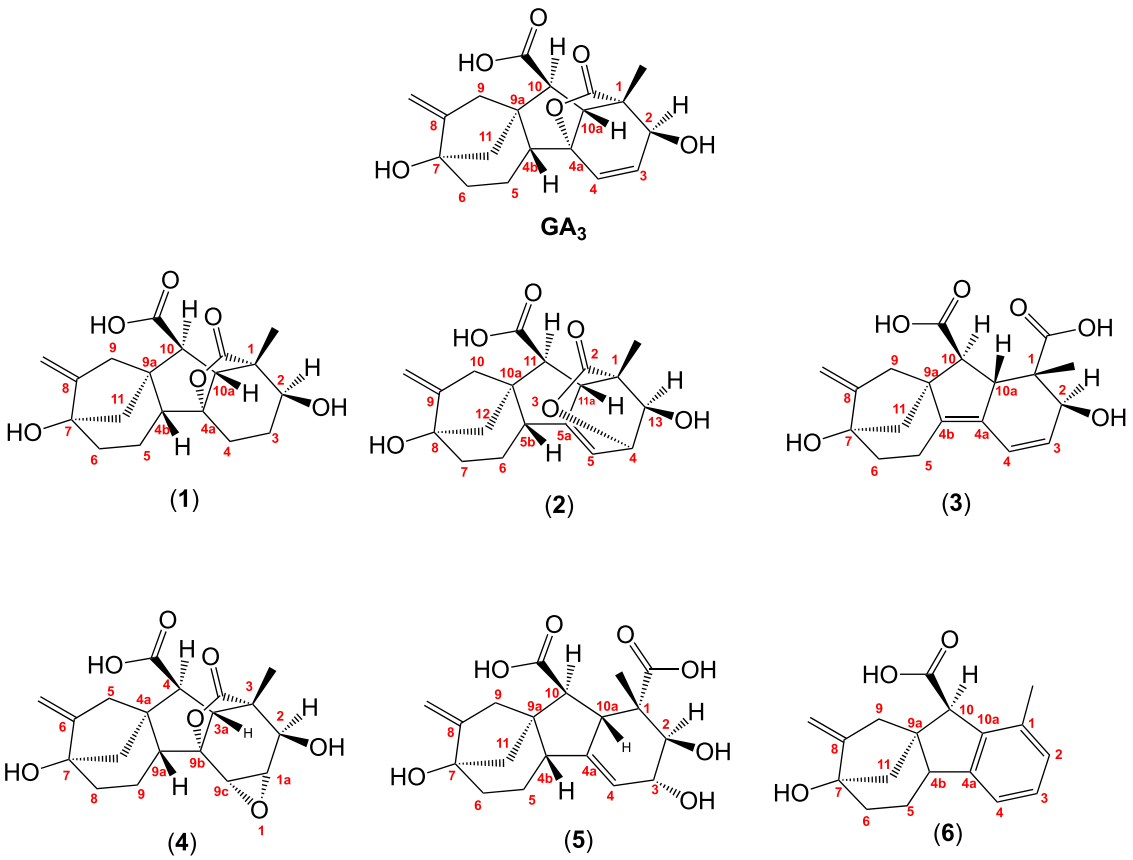

Figure 1. Chemical structure of gibberellic acid (**GA_3**), GA_1 (**1**), iso gibberellic acid (iso-GA_3) (**2**), gibberellenic acid (**3**), 1α,2α-epoxygibberellin A3 (**4**), (1α,2β,3α,4bβ,10β)-2,3,7-trihydroxy-1-methyl-8-methylenegibb-4-ene-1,10-dicarboxylic acid (**5**), and 9-bH epiallogibberic acid (**6**).

The free-binding energy of all complexes and the best poses preparatory for metadynamics simulations were calculated and selected using a molecular mechanic method (included in the Schrodinger Suite Prime module) set up on the generalized-Born surface area (MM-GBSA) with an implicit solvent and using default parameters.[25,26]

Moreover, for a comparison, IFD, MM-GBSA, and metadynamics (MTD) simulations were also carried out on **GA_3**. We applied the binding pose MTD protocol to study these docking models of GID1 in all-atom MD simulations. All MTD simulations were performed using GPUs and the Schrödinger suite Desmond tool. To efficiently evaluate the ligand stability in solution, binding pose metadynamics (BPMD), as implemented in Maestro version12.5, was performed.[27,28]

For the BPMD experiments, we performed 10 independent 10 ns MD simulations using the collective variables (CV) as a measure of the root-mean-square deviation (RMSD) of the ligand heavy atoms relative to their initial position. Alignment before RMSD calculation was performed by selecting protein residues within 3 Å from the ligand. The Ca atoms of these binding site residues were aligned with the Ca atoms in the first frame of the MTD trajectory before calculating the heavy atom RMSDs and ligand conformations in the first frame. The width and hill height were set at 0.02 Å and 0.05 kcal/mol (approximately one over 10 of the typical system thermal energy, kBT), respectively. Solvation of the system was performed in a box containing SPC/E water molecules prior metadynamics run. Then, several minimization and controlled molecular dynamics (MD) steps were carried out to allow the system to progressively get the chosen temperature of 300 K, also discharging any disadvantaged contacts and/or strains present in the preliminary structure. Subsequently, as a reference for the metadynamics production phase, we used the final snapshot of the short unbiased MD simulation of 0.5 ns.

A fundamental of BPMD is that, under the same bias forces, ligands that do not engage in stable contact with the receptor will show a greater RMSD variation in comparison to those that are firmly bound. The score provided by BPMD is associated with ligand stability during metadynamics experiments, and it is averaged over all 10 repeated simulations. The average RMSD from the initial pose is provided by the PoseScore. A rapid spread in PoseScore indicates that the ligand is not at a definite energy minimum and, thus may not be properly modeled. Structures whose contact network is undermined by the BPMD bias exhibit low PerScores. Metadynamics simulations were analyzed, and images were created with the metadynamics analysis tool embedded in the Desmond tool of the Schrodinger Suite.

RESULTS

Analytical Findings. *Identification of Impurities by HPLC−DAD, LC-QTOF-MS, and NMR Analysis.* To identify the principal gibberellic acid impurities, three commercially available batches (B1, B2, and B3) of **GA_3** were assessed by means of HPLC−DAD and LC-QTOF-MS platforms. Base peak chromatographic separation of relevant impurities was achieved by HPLC−DAD (see the Supporting Information section). Nevertheless, since UV spectra of gibberellic acid

https://doi.org/10.1021/acsomega.2c04743
ACS Omega 2023, 8, 1957−1966

impurities, with maximum absorption at 210−220 nm, were not helpful for their structural elucidations (see the Supporting Information section), additional experiments have been carried out through a QTOF-MS apparatus. Five main compounds, GA_1 (**1**), iso gibberellic acid (iso-GA_3) (**2**), gibberellenic acid (**3**), 1α,2α-epoxygibberellin A3 (**4**), and the (1α,2β,3α,4bβ,10β)-2,3,7-trihydroxy-1-methyl-8-methylene-gibb-4-ene-1,10-dicarboxylic acid (**5**) (Figure 1) were characterized by HRMS experiments (mass spectra available in the Supporting Information section). For better structural confirmation, compounds (**2**), (**3**), and (**5**) were synthesized[15] as pure standards, while compound (**4**) was commercially purchased. The 9-βH epiallogibberic acid (**6**) was also synthesized for *in silico* structural characterization purposes.

Subsequently, to separate gibberellic acid (**GA_3**) from its principal impurities (>0.1%), we developed a suitable reversed-phase HPLC method using a mobile phase containing methanol, water, and acid modifiers to provide selectivity. More specifically, the previously identified compounds were resolved from **GA_3** and each other at the gradient and isocratic conditions described in the experimental section. Using an isocratic mobile phase method as described above, **GA_3** (*rt* = 16.03 min) and its main impurities were quantified. Every detected peak was then identified by full scan mass spectrometry LC-QTOF-MS and further quantified by HPLC−DAD (n = 4). Table 1 summarizes its quantitative composition.

Table 1. Chemical Composition and Percent Contents of B1, B2, and B3 as Quantified by HPLC−DAD (n = 4)

Gibberellic acid derivatives	*rt* (min)	area % B1	area % B2	area % B3
GA_3	8.318	95.20 ± 0.07	98.09 ± 0.35	95.11 ± 0.42
(1)	8.705	2.48 ± 0.16	0.98 ± 0.14	1.09 ± 0.08
(2)	6.741	0.72 ± 0.12	0.14 ± 0.06	0.20 ± 0.05
(3)	7.648	1.38 ± 0.09	0.29 ± 0.14	0.33 ± 0.10
(4)	6.603	0.12 ± 0.05	0.12 ± 0.04	3.04 ± 0.15
(5)	6.756	0.10 ± 0.05	0.38 ± 0.06	0.23 ± 0.10

Validation of the HPLC−DAD Analysis. To validate the described method, we then proceeded to the determination of parameters such as linearity, repeatability, reproducibility, limit of detection (LOD), limit of quantification (LOQ), and recoveries, as established by the EU guidelines for HPLC-UV and LC-MS methods. Linearity was assessed by analyzing standard solutions to cover the expected range of every GA_3 and impurity concentration in the studied batches. It was studied over the range of 0.5−2.0 mg/L for **GA_3** and 5.0−100 mg/L for (**1**), (**2**), (**3**), (**4**), and (**5**). A linear relationship between peak areas of the GAs and the corresponding concentrations was found: the correlation coefficient (r^2) for **GA_3** alone and the corresponding impurities were more than 0.9991. Repeatability was, respectively, in the range of 6.5−2.7 (Table 2). For reproducibility studies for the quantification of gibberellic acid impurities by HPLC−DAD, six replicate solutions of three standard concentrations of each GA were analyzed on six different days. The corresponding RSDr values are in the range of 1.0−2.5. (Table 2) The Cochran test served to estimate the homogeneity of the variances of the repeatability and reproducibility RSDs. Results demonstrated the absence of outliers.

Table 2. HPLC Method Validation Parameters

compound	linearity	LOD (mg/L)	LOD (mg/L)	repeatability precision (%)	intraday precision (%)
GA_3	0.9997	0.95	0.56	−6.5 and 3.1	1.5 and 1.0
(1)	0.9999	1.05	0.67	−5.2 and 2.7	2.3 and 1.5
(2)	0.9999	1.56	1.01	−5.2 and 3.3	2.4 and 1.5
(3)	0.9996	0.99	0.45	−5.9 and 3.3	2.5 and 1.2
(4)	0.9991	1.35	0.74	−5.5 and 2.9	2.0 and 1.4
(5)	0.9995	3.22	2.15	−5.4 and 3.0	2.5 and 1.5

The limit of detection (LOD) for each gibberellin was determined as the sample concentration that produces a peak with a height three times the level of the baseline noise and the limit of quantification

LOQ was calculated as the sample concentration that produces a peak with 10 times the ratio of signal-to-noise. The stock standard solutions were diluted to a series of appropriate concentrations with the mobile phase, and an aliquot of the diluted solutions was injected into the HPLC−DAD instrument for analysis. LOD and LOQ values are shown in Table 2.

In Silico Findings. As previously stated, an *in silico* investigation of the structural requirements for the interactions of gibberellins with the GID1 receptor was also carried out. In detail, the study was articulated in two parts: **Part 1**. Validation of the receptor model and the ligand−receptor interactions. **Part 2**. Application of the model to the investigation of GA impurities.

Part 1. GID1 protein was acquired from an online protein databank based on its resolution and the electron density map. Subsequently, after optimization and energy minimization, the protein has been analyzed by means of the Maestro Protein Reliability Report. The comparison with the original diffraction data confirmed its accuracy, a prerequisite for docking experiments.

A cross-docking approach was then applied to **GA_3** and **GA_4** crystallographic ligands (PubChem CIDs 92109 and 6466, respectively) for a more successful prediction of the ligand-binding pose. In fact, a ligand−receptor complex solved in the presence of a single specific ligand might reveal a lower affinity for a different ligand.[16] Thus, an IFD protocol that addresses flexibility to both the ligand and protein was chosen to predict accurate ligand-binding modes and simultaneous structural changes in the receptor, particularly important when docking structurally related ligands within different conformations of the same protein. As a result, the cross-docking experiment identified the 2ZSI as the optimal protein with the lower RMSD values and the best docking and MM-GBSA scores.

Model investigation evidenced the complete overlap of both Glide and IFD best poses with the crystallographic ligands, allowing us to identify the crucial ligand−receptor areas of interaction. Moreover, with the IFD protocol, we observed an improvement in ligand−receptor complexes' free energy, also evidencing a better correspondence of ligand−protein contacts.

Figure 2A shows the prevalence of the hydrophobic interactions (gray spheres) that characterize the receptor shape. In particular, docking images evidenced many hydrophobic interactions between the diterpenic core of the ligand and the inner part of the receptor pocket (Figure 2B).

The strongest interactions involved residues Ile24, Phe 27, Lys 28, and Tyr 31 located on the first helix. Other minor hydrophobic interactions passed between the ligand and a

https://doi.org/10.1021/acsomega.2c04743
ACS Omega 2023, 8, 1957−1966

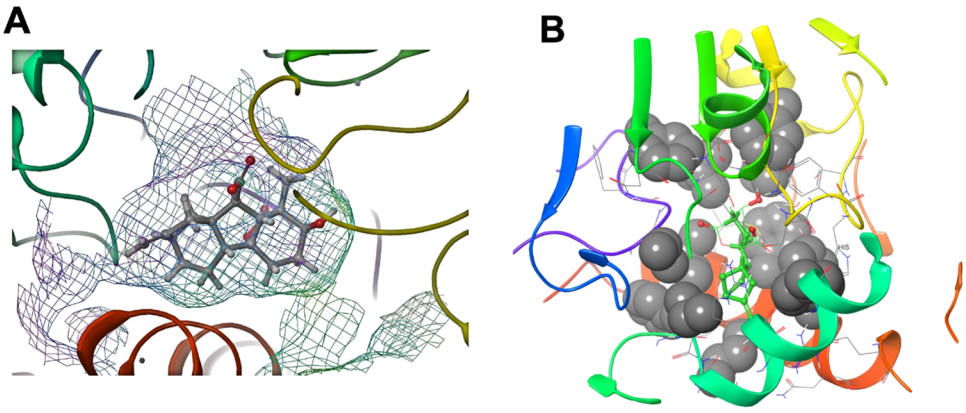

Figure 2. (A) GID1 binding site shape. (B) Hydrophobic interactions between the ligand and the receptor.

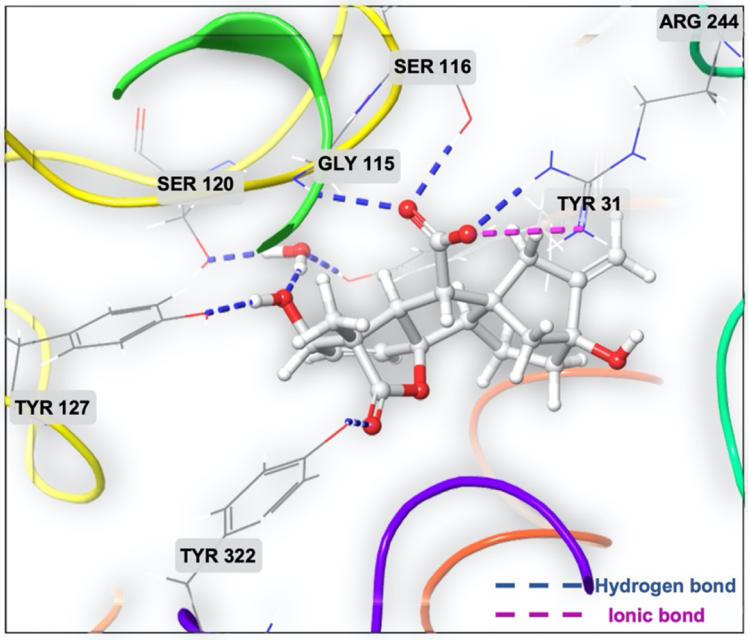

Figure 3. GID1/ GA_3 electrostatic interactions within the receptor-binding site.

Table 3. Glide/XP, IFD, MM-GBSA, and MTD/Pose Scores for the Crystallographic Ligands (GA_3 and GA_4) and Gibberellin Derivatives (1)−(6)

compound	Glide/Xp (Kcal/mol)	IFD (Kcal/mol)	MM-GBSA (Kcal/mol)	MD/posescore (Å)
GA_4	−12,229	−884,14	−75,79	n.d.
GA_3	−13,935	−885,76	−73,19	0.586
(1)	−13,496	−885,93	−75,26	n.d.
(2)	−11,999	−883,38	−74,39	0.793
(3)	−13,397	−885,85	−54,89	1.071
(4)	−13,484	−884,33	−74,60	0.945
(5)	−13,990	−885,06	−39,81	0.875
(6)	−12,244	−883,42	−50,47	1.172

series of amino acids as Arg 35, Gly, 114, Gly 115, Ser 116, Ile 126, Tyr 27, Ser 191, Phe 238, Val 239, Arg 244, Val 319, Gly 320, Tyr 322, and Leu 323. Some relevant electrostatic contacts are also present. The most relevant involves the ionic interaction between the negatively charged oxygen of the carboxyl group in 10 and the iminic nitrogen of Arg 244, together with a series of hydrogen bonds between the carbonyl oxygen of the carboxyl group in 10 position and Gly 115, Ser 116, and Ser 191, the hydroxy group in 2 position and Tyr 127, the negatively charged oxygen of carboxyl group in 10 position and Arg 244, and the carbonyl oxygen of lactone and Tyr322. Interestingly, the presence of a water molecule inside the binding pocket permitted the formation of an additional bridge contact between the ligand and the receptor, particularly

https://doi.org/10.1021/acsomega.2c04743
ACS Omega 2023, 8, 1957−1966

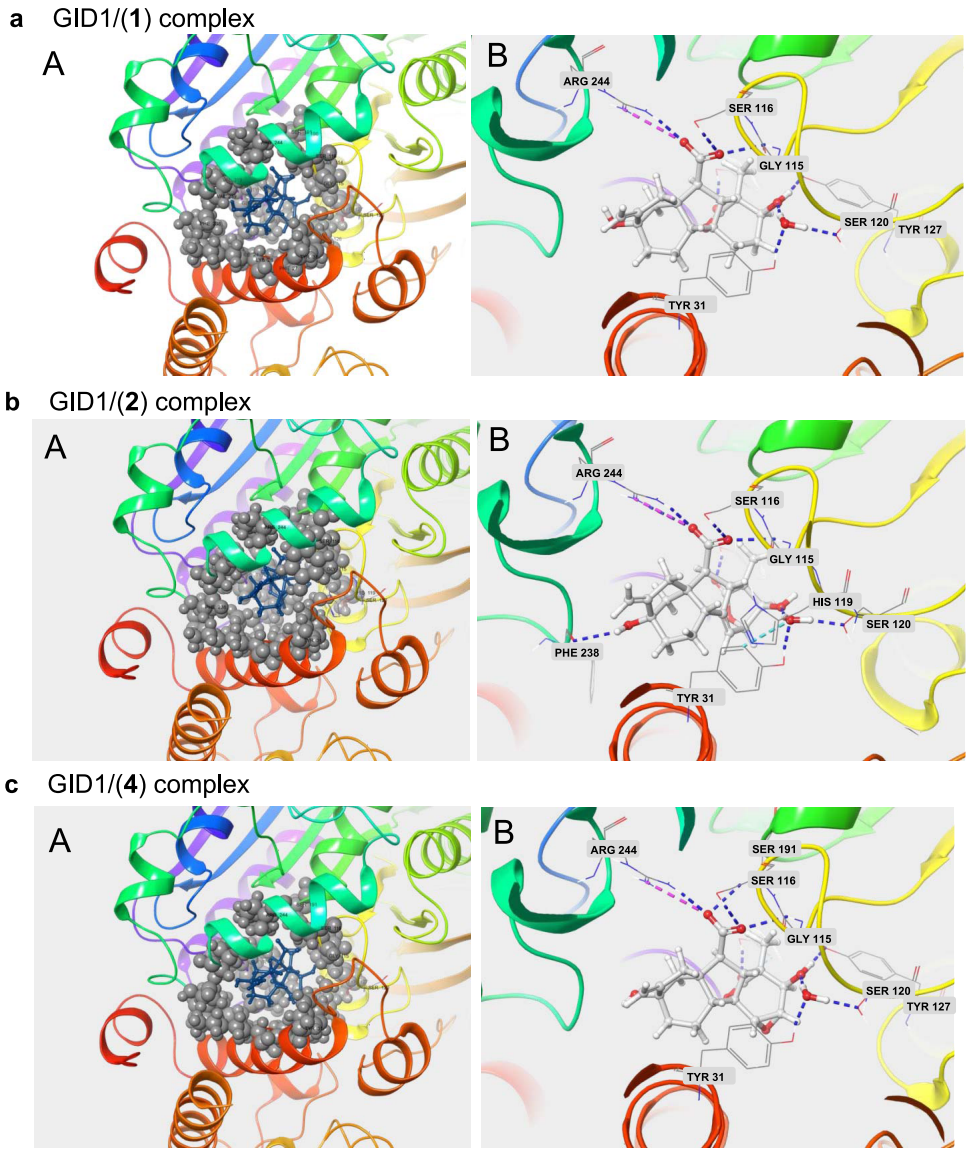

Figure 4. Binding site molecular models of GID1/(**1**), GID1/(**2**), and GID1/(**4**) complexes and representation of the hydrophobic (A) and electrostatic (B) interactions.

involving the hydroxy group in the 2 position and Tyr31 and Ser120 residues. (Figure 3)

Part 2. The molecular changes induced by the gibberellins (**1**), (**2**), (**3**), (**4**), (**5**), and (**6**) when bound to GID1, in comparison with $\mathbf{GA_3}$, were then investigated. In particular, this second part of the *in silico* study was carried out for a better characterization of the GID1 receptor-binding pocket and to investigate the receptor affinity of the selected gibberellins.

Docking studies were performed by the IFD and the extra-precision (XP) protocol embedded in Schrödinger to identify the potential pose in the receptor site for each gibberellin. Then, Prime-MM/GBSA algorithm was applied to select the best binding positions to discard the metastable or less energetically favorable poses. Table 3 shows the Glide/Xp, IFD, MM-GBSA, and MD/PoseScore values.

From a structural perspective, the absence, or the ring walking of the endocyclic double bond seemed not to affect the energy of gibberellin−receptor complexes (**1**) and (**2**) with respect to their precursor. Similarly, the introduction of the epoxide group, as in compound (**4**), did not affect the MM/GBSA scores. Conversely, lactone residue dramatically influenced the ligand-binding affinity. In fact, the hydrolysis of the $\mathbf{GA_3}$ ester group gave compound (**5**) that showed the lowest MM/GBSA score. Also, the introduction of a flat aromatic ring instead of the bulkier cyclohexene did not appear energetically favorable.

Application of the GID1 model to the investigation of the $\mathbf{GA_3}$ derivatives allowed us to identify the crucial ligand−receptor areas of interaction (LRIs). In more detail, compounds with the best MM-GBSA scores (**1**), (**2**), and (**4**) displayed the same hydrophobic and electrostatic contacts as $\mathbf{GA_3}$. Interestingly, only the interaction between the hydroxy group in the 2 position and Tyr 127 was missing in compounds (**2**) and (**4**). A novel contact between the hydroxy group adjacent to methylene and Phe 238 was also observed for compound (**2**). (Figure 4a−c).

It is worth noting that the MM-GBSA last-placed compound (**5**), albeit exhibiting a similar pose and interactions as (**1**), (**2**), and (**4**), did not engage the ionic bonding between the

https://doi.org/10.1021/acsomega.2c04743
ACS Omega 2023, 8, 1957−1966

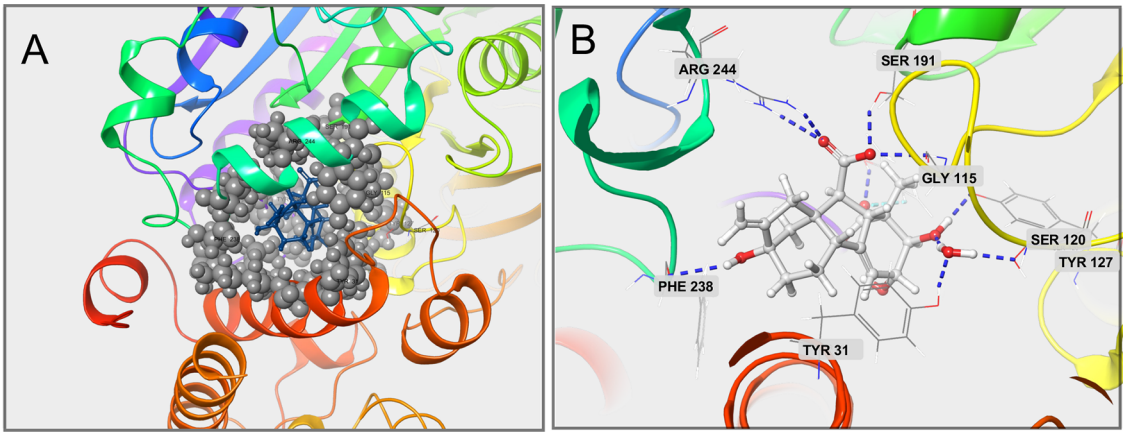

Figure 5. Binding site molecular model of the GID1/(**5**) complex and representation of the hydrophobic (A) and electrostatic (B) interactions.

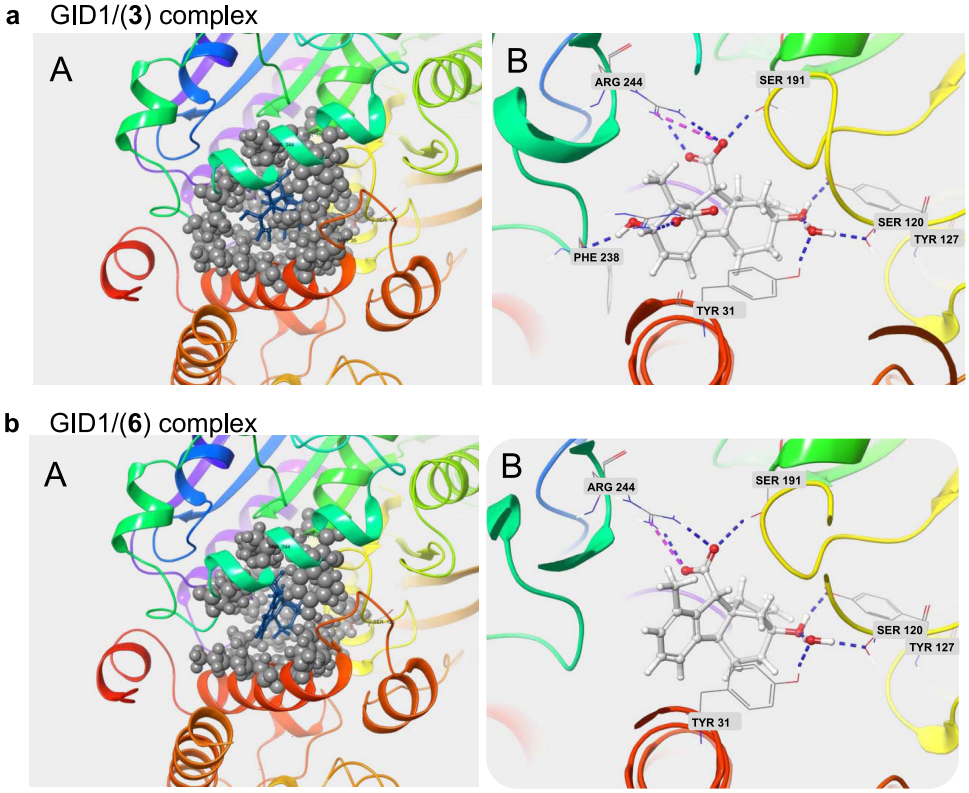

Figure 6. Binding site molecular model of GID1/(**3**) and GID1/(**6**) complexes and representation of the hydrophobic (A) and electrostatic (B) interactions.

negatively charged oxygen of the carboxyl group in 10 and the iminic nitrogen of Arg 244. (Figure 5)

Conversely, compounds (**3**) and (**6**), although engaging many of the electrostatic contacts, were not able to interact with a portion of the receptor, also assuming a different orientation within the binding pocket. A possible explanation might be related to the lack of hydrogen bonds between the ligands and Gly 115, Ser 116, Tyr 127, and Tyr322. (Figure 6a,b)

Subsequently, to better rationalization of our evidence, we investigated the structural rearrangements of the ligand−receptor complexes, which arose from the IFD experiments in light of the metadynamics simulations (MTD) carried out on a GID1 crystal. **GA_3** and the other gibberellins under study showed a high permanence of the interactions throughout the MTD experiments, also revealing a low degree of motion within the receptor (Figure 7). This is in accordance with the good stability of the compounds and corroborates the docking scores.

As expected **GA_3**, with an RMSD value of 0.586 Å, was the most stable compound. Gibberellins (**3**) and (**6**), in which the electrostatic interaction with Gly 115 and Ser 116 is missing, displayed the lowest RMSD scores of 1071 and 1172 Å, respectively, while gibberellins (**2**), (**4**), and (**5**) showed RMSD values in between 0.793 Å, 0.945 Å, and 0.875 Å, respectively (Table 3).

Biological Findings. Based on *in silico* findings, we decided to test the percent growth of tomato plants after treatment with gibberellic impurity (**2**). Tomato plants cv. Ciliegino were used to evaluate the percent growth after gibberellic acids

https://doi.org/10.1021/acsomega.2c04743
ACS Omega 2023, 8, 1957−1966

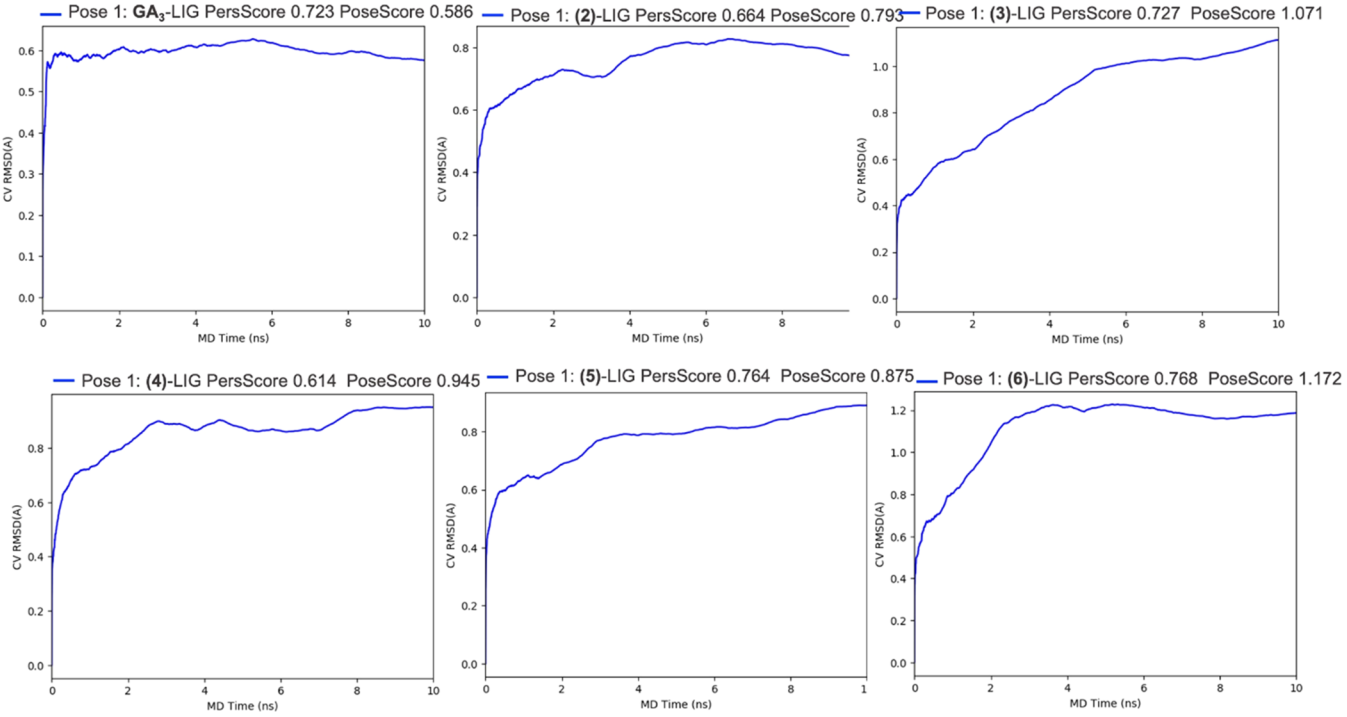

Figure 7. MTD simulations of GA_3, (2), (3), (4), (5), and (6). The plot represents the average RMSD of the ligand during the 10 × 10 ns metadynamics runs in PDB: 2ZSH (blue line). The PoseScore values are of 0.586 angstroms for GA_3, 0.793 angstroms for (2), 1.071 angstroms for (3), 0.945 angstroms for (4), 0.875 angstroms for (5), and 1.172 angstroms for (6).

treatment. Plants were sprayed with (GA_3) and (2) at a concentration of 5 mg/L using a small atomizer and taking care to avoid the soil during the treatment. Tween 20 was used as a reference compound. The experiment comprised 12 plants, four per treatment. From 14 days after the first spray, growth was assessed by measuring the stem heights from the cotyledonary node. We found that the compounds (2) and (GA_3) exerted plant growth of 5.12 and 16.2%, respectively.

DISCUSSION AND CONCLUSIONS

A simple and straightforward HPLC method with DAD and MS detection has been successfully developed to determine gibberellic acid and its impurities in a technical sample. In this work, three impurities in the gibberellic acid bulk sample were identified as GA_1 (1), iso gibberellic acid (iso-GA_3) (2), gibberellenic acid (3), 1α,2α-epoxygibberellin A3 (4), and (1α,2β,3α,4bβ,10β)-2,3,7-trihydroxy-1-methyl-8-methylene-gibb-4-ene-1,10-dicarboxylic acid (5) (see the Supporting Information section). Specificity, linearity, sensitivity, precision, and accuracy were measured and discussed. The method was also used to quantify these impurities in three technical samples. The method developed herein should be applicable with minor modifications for gibberellic acid quality control and assurance in future investigations.

Based on IFD, MM-GBSA data, and MTD simulations, all of the gibberellins under study, apart from (5) and (6), assumed similar orientation and stability inside the receptor, with compounds (1), (2), and (4) displaying energetically more favorable ligand−receptor complexes related to a better adaptation to the GID1 volume and hydrophobic environment and to the various important electrostatic interactions that they engage with the pocket itself. Interestingly, the electrostatic contacts with Gly 115 and Ser 116 residues play a key role to stabilize the ligands within the receptor, also reducing the free energy of the ligand−receptor complex itself. Moreover, the strong ionic bond with Arg 244 seemed to be important to make the complex energetically more rather than to the stabilization of the ligand inside the pocket.

Based on these *in silico* assumptions, we speculate that all of the investigated gibberellin derivatives might exert a biological activity similar to GA_3, with (2) and (4) the most promising hit to lead compounds.

Our preliminary biological experiment carried out on tomato plants indicated that compound (2) might act as a plant hormone, although with a plant growth rate lower than technical gibberellic acid GA_3.

ASSOCIATED CONTENT

Supporting Information

The Supporting Information is available free of charge at https://pubs.acs.org/doi/10.1021/acsomega.2c04743.

HRMS spectra of GA_3, (1), (2), (3), (4), and (5); ^{1}H and ^{13}C NMR spectra of compounds (2), (3), (5), and (6); GA_3 ligand−2ZSI receptor and GA_4 ligand−2ZSI interactions for (1) crystal ligand, (2) glide best pose, and (3) IFD best pose; docking and free-binding energy scores for compounds (1)−(6) and MTD simulations of GA_3 and compounds (2)−(6); HPLC−DAD and UV spectra of GA_3, (1), (2), (3), (4), and (5); and photo of tomato plants after 14 days of treatment with reference Tween 20, compound (2), and GA_3 (PDF)

AUTHOR INFORMATION

Corresponding Authors

Pierluigi Caboni − *Department of Life and Environmental Sciences, Cittadella Universitaria di Monserrato, 09042*

https://doi.org/10.1021/acsomega.2c04743
ACS Omega 2023, 8, 1957−1966

Monserrato, Italy; orcid.org/0000-0003-2448-3767; Email: caboni@unica.it

Graziella Tocco − *Department of Life and Environmental Sciences, Cittadella Universitaria di Monserrato, 09042 Monserrato, Italy;* orcid.org/0000-0003-0081-5704; Email: toccog@unica.it

Authors

Antonio Laus − *Department of Biomedical Sciences, Cittadella Universitaria di Monserrato, 09042 Monserrato, Italy*

Kodjo Eloh − *University of Kara, 404 Kara, Togo*

Nikoletta G. Ntalli − *Department of Pesticides Control and Phytopharmacy, Benaki Phytopathological Institute, 14561 Athens, Greece*

Mattia Casula − *Department of Life and Environmental Sciences, Cittadella Universitaria di Monserrato, 09042 Monserrato, Italy*

Sabrina Di Giorgi − *Ministero della Salute, Direzione Generale per l'Igiene e la Sicurezza degli Alimenti e della Nutrizione, 00144 Roma, Italy*

Complete contact information is available at: https://pubs.acs.org/10.1021/acsomega.2c04743

Author Contributions

P.C. and G.T. designed the study and supervised, wrote, and edited the manuscript. A.L. planned, performed, and analyzed *in silico* experiments and data. G.T. carried out synthetic and structural characterization experiments. K.E. and M.C. performed analytical experiments. N.N. and S.D.G. reviewed and edited the manuscript.

Notes

The authors declare no competing financial interest.

■ ACKNOWLEDGMENTS

Dedicated to the memory of Professor Lewis Norman Mander (1939−2020).

■ REFERENCES

(1) Machado, M. C.; Soccol, C. R. Gibberellic Acid Production. In *Current Developments in Solid-state Fermentation*; Pandey, A.; Soccol, C. R.; Larroche, C., Eds.; Springer: New York, 1996; pp 277−301 DOI: 10.1007/978-0-387-75213-6_13.

(2) Rachev, R. C.; Pavlova-Rouseva, R.; Bojkova, S.; Gancheva, V. Isolation of gibberellic acid produced by Fusarium moniliforme. *J. Nat. Prod.* **1993**, *56*, 1168−1170.

(3) EPA, U. Gibberellic Acid: Reregistration Eligibility Decision (RED) Fact Sheet ARCHIVES. https://archive.epa.gov/pesticides/reregistration/web/pdf/4110fact.pdf, 1995.

(4) Castillo, G.; Martinez, S. Reversed-phase C18 high-performance liquid chromatography of gibberellins GA3 and GA1. *J. Chromatogr. A* **1997**, *782*, 137−139.

(5) Directorate-General, E. H. A. C. Gibberellic acid SANCO/2613/08 − rev. 107 July 2008 rev. 21 June, 2012, http://ec.europa.eu/food/plant/pesticides/eu-pesticidesdatabase/public/?event=activesubstance.ViewReview&id=537.

(6) Germany, Z. R. M. S. Extension of Authorisation for Minor Uses. https://www.bvl.bund.de/SharedDocs/Downloads/04_Pflanzenschutzmittel/01_zulassungsberichte/005879-00-01.pdf?__blob=publicationFile&v=2, February 12, 2013.

(7) E.F.S.A.. Conclusion on the peer review of the pesticide risk assessment of the active substance gibberellic acid (GA3). *EFSA J.* **2012**, *10*, 2507.

(8) Ambrus, A.; Hamilton, D. J.; Kuiper, H. A.; Racke, K. D. Significance of Impurities in the Safety Evaluation of Crop Protection Products. *Pure Appl. Chem.* **2003**, *75*, 937−973.

(9) Public consultation on the active substance gibberellic acid | EFSA (europa.eu), 2019, https://www.efsa.europa.eu/en/consultations/call/190522.

(10) Lin, J. T.; Stafford, A. E. Reversed-phase C18 and normal-phase silica high-performance liquid chromatography of gibberellins and their methyl esters. *J. Chromatogr. A* **1988**, *452*, 519−525.

(11) Han, Z.; Liu, G.; Rao, Q.; Bai, B.; Zhao, Z.; Liu, H.; Wu, A. A liquid chromatography tandem mass spectrometry method for simultaneous determination of acid/alkaline phytohormones in grapes. *J. Chromatogr. B* **2012**, *881−882*, 83−89.

(12) Davière, J.-M.; Achard, P. A pivotal role of DELLAs in regulating multiple hormone signals. *Mol. Plant* **2016**, *9*, 10−20.

(13) Murase, K.; Hirano, Y.; Sun, T. P.; Hakoshima, T. Gibberellin-induced DELLA recognition by the gibberellin receptor GID1. *Nature* **2008**, *456*, 459−463.

(14) Shimada, A.; Ueguchi-Tanaka, M.; Nakatsu, T.; Nakajima, M.; Naoe, Y.; Ohmya, H.; Kato, H.; Matsuoka, M. Structural basis for gibberellin recognition by its receptor GID1. *Nature* **2008**, *456*, 520−523.

(15) Huigens, R. W., III; Morrison, K.; Hicklin, R.; Flood, T. A.; Richter, M. F.; Hergenrother, P. J. A ring-distortion strategy to construct stereochemically complex and structurally diverse compounds from natural products. *Nat. Chem.* **2013**, *5*, 195−202.

(16) *Schrödinger Release 2021-1: Maestro*; Schrödinger, LLC: New York, NY, 2021.

(17) Madhavi Sastry, G.; Adzhigirey, M.; Day, T.; Annabhimoju, R.; Sherman, W. Protein and ligand preparation: parameters, protocols, and influence on virtual screening enrichments. *J. Comput. Aided Mol. Des.* **2013**, *27*, 221−234.

(18) *Schrödinger Release 2021-1: Protein Preparation Wizard; Epik, Schrödinger, LLC, New York, NY, 2021; Impact, Schrödinger, LLC, New York, NY; Prime*; Schrödinger, LLC: New York, NY, 2021.

(19) Harder, E.; Damm, W.; Maple, J.; Wu, C.; Reboul, M.; Xiang, J. Y.; Wang, L.; Lupyan, D.; Dahlgren, M. K.; Knight, J. L.; Kaus, J. W.; Cerutti, D. S.; Krilov, G.; Jorgensen, W. L.; Abel, R.; Friesner, R. A. OPLS3: A Force Field Providing Broad Coverage of Drug-like Small Molecules and Proteins. *J. Chem. Theory Comput.* **2016**, *12*, 281−296.

(20) *Schrödinger Release 2021-1: LigPrep*; Schrödinger, LLC: New York, NY, 2021.

(21) Greenwood, J. R.; Calkins, D.; Sullivan, A. P.; Shelley, J. C. Towards the comprehensive, rapid, and accurate prediction of the favorable tautomeric states of drug-like molecules in aqueous solution. *J. Comput. Aided Mol. Des.* **2010**, *24*, 591−604.

(22) *Schrödinger Release 2021-1: Epik*; Schrödinger, LLC: New York, NY, 2021.

(23) *Schrödinger Release 2021-1: Induced Fit Docking protocol; Glide, Schrödinger, LLC, New York, NY, 2021; Prime*; Schrödinger, LLC: New York, NY, 2021.

(24) Sherman, W.; Day, T.; Jacobson, M. P.; Friesner, R. A.; Farid, R. Novel procedure for modeling ligand/receptor induced fit effects. *J. Med. Chem.* **2006**, *49*, 534−553.

(25) *Schrödinger Release 2021-1: Prime*; Schrödinger, LLC: New York, NY, 2021.

(26) Ylilauri, M.; Pentikäinen, O. T. MMGBSA as a tool to understand the binding affinities of filamin-peptide interactions. *J. Chem. Inf. Model.* **2013**, *53*, 2626−2633.

(27) *Schrödinger Release 2021-1: Desmond Molecular Dynamics System, D. E. Shaw Research*; Maestro-Desmond Interoperability Tools, Schrödinger: New York, NY, 2021.

(28) Fusani, L.; Palmer, D. S.; Somers, D. O.; Wall, I. D. Exploring Ligand Stability in Protein Crystal Structures Using Binding Pose Metadynamics. *J. Chem. Inf. Model.* **2020**, *60*, 1528−1539.